
PERGAMON

Journal of Quantitative Spectroscopy & Radiative Transfer 82 (2003) 133–150

Journal of Quantitative Spectroscopy & Radiative Transfer

www.elsevier.com/locate/jqsrt

Retrieval of atmospheric water vapor columns from FT visible solar absorption spectra and evaluation of spectroscopic databases

Pierre-François Coheur[a,*,1], Cathy Clerbaux[a,2], Michel Carleer[a], Sophie Fally[a], Daniel Hurtmans[a], Réginald Colin[a], Christian Hermans[b], Ann Carine Vandaele[b], Brice Barret[b], Martine De Mazière[b], Hugo De Backer[c]

[a] *Laboratoire de Chimie Quantique et Photophysique, Université Libre de Bruxelles, 50 Av. F.D. Roosevelt, B-1050 Brussels, Belgium*

[b] *Belgian Institute for Space Aeronomy (BIRA-IASB), Av. Circulaire 3, B-1180 Brussels, Belgium*

[c] *Royal Meteorological Institute (KMI-IRM), Av. Circulaire 3, B-1180 Brussels, Belgium*

Received 7 February 2003; received in revised form 18 March 2003; accepted 22 March 2003

Abstract

The absorption of solar light by atmospheric water vapor in the visible spectral region is analyzed by means of ground-based absorption Fourier transform spectroscopy, performed at high resolution in Brussels during summer 2001. Several microwindows between 14,000 and 18,000 cm^{-1}, in which water vapor lines are well isolated from solar lines and other atmospheric trace gases absorptions, are examined. They are demonstrated to be adequate for the retrieval of the total water vapor column. Based on the retrievals, a detailed analysis of the water vapor line parameters published in the HITRAN database and recently reinvestigated by different groups is performed. The analysis focuses on the one hand on the comparison of the retrieved water vapor columns with in situ measurements, performed at the same time as the spectroscopic measurements and at the same location, and on the other hand on the quality of the spectral fits. It is shown that the discrepancies between the line lists affect significantly the results. In particular it is shown that the weaker lines, not measured in earlier laboratory experiments, do contribute at large zenith angles and need to be taken into account in order to better simulate the atmospheric spectra. The importance of the pressure broadening parameters is also highlighted.

Keywords: Water vapor; Line parameters; Atmospheric radiation

* Corresponding author. Fax: +32-2-6504-232.

E-mail address: pfcoheur@ulb.ac.be (P.-F. Coheur).

[1] P.-F. Coheur is Scientific Research Worker with the Fonds National de la Recherche Scientifique.

[2] Also at Service d'Aéronomie, Université de Paris 6, Paris, France.

0022-4073/03/$ - see front matter © 2003 Elsevier Ltd. All rights reserved.
doi:10.1016/S0022-4073(03)00150-X

1. Introduction

The spectroscopic properties of water vapor, recently reviewed [1], are of crucial importance in astronomy and in atmospheric sciences. Water vapor is for example responsible for 70% of the atmospheric absorption of the incoming solar radiation and for most of the outgoing infrared radiation of the Earth's surface [2]. This results in a significant heating of the atmosphere, which is essential to the existence of life on Earth.

The radiative properties of water vapor in the Earth's atmosphere are tightly related to the rotation–vibration spectrum of the water molecule, which covers a spectral interval from the infrared to the near ultraviolet. The infrared spectrum is very intense and has been analyzed thoroughly in the laboratory, using several experimental techniques, and by theory (see [1] and references therein). The line parameters in the infrared are readily available in spectroscopic databases, both for strong and weak lines. In the visible and near-ultraviolet regions, one is concerned with overtone bands, which have a weaker intensity. The measurement of the water vapor line parameters in the latter spectral regions requires therefore very long optical paths, which are most frequently obtained in the laboratory by using White-type multiple reflection cells [3–8] or by using intracavity laser absorption or cavity-ring-down spectroscopies [9–12]. The weak water lines can also be measured in the atmosphere, for example in solar spectra recorded from the ground [13]. Among these different techniques, the major advances have been made using long path cells and high-resolution Fourier transform spectrometers, which, despite a lower sensitivity as compared to the laser spectroscopic methods, overcome the problems of calibration and allow measuring simultaneously over a wide spectral interval.

The first high-resolution absorption spectrum of water vapor obtained following this technique was recorded using the McMath Fourier transform spectrometer at the Kitt Peak National Observatory [3,4]. Many lines were identified and assigned in the spectral range between 13,200 and 25,000 cm^{-1}, and accurate positions and intensities were measured. These parameters were compiled to form the basis of the HITRAN spectroscopic database for water vapor in the visible region. Several improvements were later brought to HITRAN with the inclusion of some measured broadening parameters [3,4,14,15]. Problems with the line intensities in HITRAN 96 were highlighted by Giver et al. [16] and corrected in the latest (HITRAN 2000) version of this database [17].

The need for improving even more the spectroscopic parameters for water vapor in the visible spectral range has become evident through recent research on the role played by water vapor in the climate system. It was for example suspected that weak water lines, not measured in the earlier experiments, could contribute significantly to the Earth's energy balance [18–20]. More recently, it was also demonstrated that the water vapor total columns and eventually the vertical profiles could be retrieved from satellite-borne spectrometers operating in the visible region (e.g. GOME and SCIAMACHY), with an accuracy similar to that of the more frequently used infrared and microwave spectrometers [21,22]. In these studies, a significant part of the uncertainties in the calculated quantities (radiative fluxes or water vapor columns) were found to originate in the lack of precise spectroscopic data. Two experiments, similar to that of the Kitt peak measurements [3,4], have been conducted recently by independent groups of researchers with the objective of improving the water vapor line parameters, both by improving the assignment of weaker lines and by the measurement of the pressure-dependent parameters (widths and positions). One of the two experiments was carried out at the Rutherford Appleton Laboratory (RAL) Molecular Spectroscopy Facility under the auspices of the European Space Agency (ESA) and the other was conducted at the University of

Reims, in partnership with Belgian institutions. Both experiments yielded a new water vapor line list (available at http://www.msf.rl.ac.uk/ and http://www.ulb.ac.be/cpm), which significantly improves the HITRAN database from the point of view of the number of measured lines and the assignments. The first line list will be referred to as the ESA database [7,8] and the other as the Bxl-Reims database (hereafter BR) [5,6,23]. Several studies have already reported on the differences between HITRAN and these new line lists, and on how these differences affect on atmospheric calculations. In most of these studies, the main objective was to analyze how the changes in the databases influence the Earth's energy balance [18,19,24] but in other studies, attention was paid to the reliability of the databases for modeling atmospheric spectra [21,25–27]. This was for example done when studying the retrieval of water vapor columns from the GOME nadir-looking satellite spectra [21]. For this study, a small spectral interval ($16{,}666$–$17{,}094\ \mathrm{cm}^{-1}$) containing water vapor lines with a moderate intensity, sensitive to pressure and temperature effects, was chosen. The results showed that the sources of errors in the retrievals of the water vapor columns were due in part to the low-resolution of the GOME instrument (0.27 nm or $7.7\ \mathrm{cm}^{-1}$ Full-Width at Half-Maximum), which did not allow the proper identification and modeling of all sources of extinction (due to aerosols, $O_2.O_2$ complexes, NO_2, Fraunhofer lines) in the spectral range considered [21]. Veihelmann et al. [27] describe a similar study using atmospheric spectra recorded from the ground with a Fourier transform spectrometer operating at a higher spectral resolution ($0.05\ \mathrm{cm}^{-1}$). The analysis was performed in the spectral range useful for GOME ($16{,}666$–$17{,}094\ \mathrm{cm}^{-1}$) and focuses on the reliability of the water vapor line lists for modeling the atmospheric spectra. The authors conclude that the spectra simulated with the HITRAN2000 and the BR databases provide a good agreement with the observations. A slightly better agreement over the entire spectral region investigated was, however, obtained with HITRAN2000, whereas the intensities of well-defined water lines were better accounted for with the BR line list. In Veihelmann et al. [27], a single spectrum was analyzed and the atmospheric calculations were based on forward radiative transfer calculations only.

In the present work, we intend to go further in testing the reliability of the water vapor spectroscopic databases for atmospheric remote-sensing purposes. To do this, we analyzed an extensive series of high-resolution Fourier transform spectra recorded from the ground during a measurement campaign held in Brussels in June 2001. Five atmospheric windows were investigated to extend the comparison of the water vapor line lists given in references [26,27] to the spectral range between $14{,}000$ and $18{,}000\ \mathrm{cm}^{-1}$. The analysis is performed by using forward radiative model simulations along with an inversion algorithm to retrieve the total water vapor column. This allows us to investigate the quality of the water vapor line lists on a relative basis (comparison of the quality of the spectral fittings and homogeneity of the retrieved water vapor columns over the different spectral ranges investigated) and on an absolute basis (comparisons with collocated sonde measurements). The experimental conditions and retrieval algorithm are described in the two next sections of this paper. In Section 4, the results are presented and discussed. A brief summary of the spectroscopic parameters available from the different databases is also given. Conclusions are provided in Section 5.

2. Experimental

The solar absorption spectra analyzed here were recorded in Brussels (4.358°E, 50.798°N) during a 1-month campaign in June 2001. The spectrometer was a Bruker IFS120M Fourier transform

spectrometer, which was operated in the visible spectral range at a spectral resolution of 0.1 cm^{-1} (9 cm MOPD), using a quartz beamsplitter, a silicon diode detector and a blue-green filter. Sixteen interferograms were co-added within a total measurement time of 5 min, and yielded spectra with a good signal-to-noise ratio (~ 250). For the present work, we have analyzed the spectra recorded during two clear-sky days in June (25th and 26th), which provided measurements from sunrise to sunset, thus allowing the analyses of data recorded at low- and at high-solar zenith angles.

During these two days, balloon-borne PTU sondes were launched by the Royal Meteorological Institute, at 12h00 (GMT). These measurements provide pressure, temperature and relative humidity vertical profiles from the ground up to about 10 km with a good vertical sampling resolution (50–70 m depending on the ascending speed of the balloon). The estimated uncertainty on the relative humidity, measured with a Vaisala RS90 sonde, was 5% (2σ).

3. Data analysis

A raw solar absorption spectrum, measured at a solar zenith angle of 69.03°, is given in Fig. 1. From this figure it is seen that the solar lines dominate most of the spectrum above 18,000 cm^{-1}.

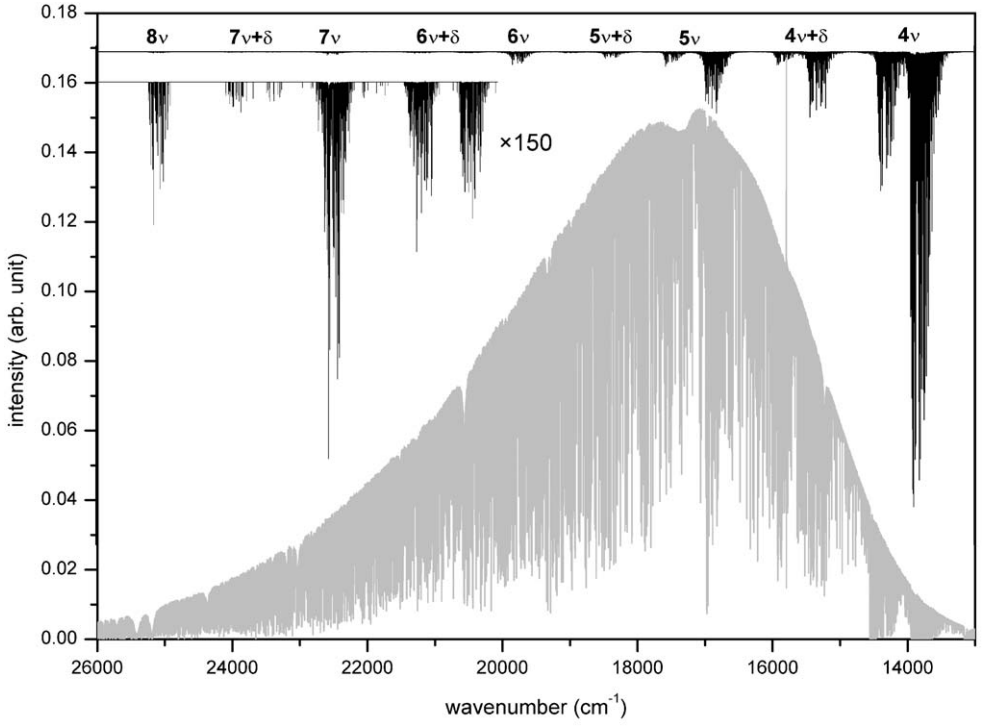

Fig. 1. Solar absorption spectrum (gray line) recorded in Brussels (4.358°E, 50.798°N) at 0.1 cm^{-1} resolution, on the 25th of June 2001. The black line shows the simulation of the water vapor atmospheric absorption (1 atm of air) at the same spectral resolution.

Table 1
Atmospheric windows and exclusion ranges selected for retrieving water vapor columns from the FT visible solar absorption spectra

	ν_{low} (cm^1)	ν_{high} (cm^{-1})	$\Delta\nu$ (cm^{-1})	Exclusion ranges in the fit (cm^{-1})
Atmospheric window				
1	14,288.1	14,320.0	31.9	14,295.9–14,297.4
				14,304.9–14,305.8
2	15,319.0	15,335.6	16.6	—
				15,417.6–15,425.0
3	15,400.0	15,450.0	50.0	15,437.0–15,438.6
				15,446.8–15,450.0
4	16,809.7	16,819.7	10.0	—
				16,880.7–16,882.1
5	16,876.3	16,897.6	21.3	16,891.0–16,892.6

The water vapor bands are strongest in the lowest energy part of the spectrum and saturation is important below $14,000\ cm^{-1}$, especially at large zenith angles. We have therefore restricted the present analysis to the $14{,}000–18000\ cm^{-1}$ region, which covers part of the 4ν, $4\nu+\delta$ and 5ν polyads of the water vapor absorption spectrum (Fig. 1). In that spectral range, five atmospheric windows in which few solar lines interfere with the water vapor absorption lines were further selected for retrieving the total water vapor columns (Table 1).

The retrievals were performed using an inversion algorithm developed by two of us (D.H. and M.DM.), which relies on a widely used forward radiative transfer model (FSCATM [28]) for the calculation of the geometry and the initial atmospheric state. The algorithm, which participated successfully in an intercomparison exercise initiated by the NDSC [29], works as follows: a synthetic spectrum is obtained by multiplying the molecular transmittances for each molecule and for the different atmospheric layers according to the average local temperature and pressure conditions. This spectrum is then convoluted by the instrumental line shape and fitted to the observed spectrum. The shapes of the vertical distributions of the targeted species are kept fixed and only the column or partial-columns are adjusted by globally multiplying the corresponding concentrations. The baseline of the spectrum is also adjusted. The fitting algorithm is a modified Levenberg–Marquardt non-linear least-squares procedure [30] providing a straightforward estimation of the statistical error made on each determined molecular amount. Several portions of the spectral interval, which contain for instance strong solar lines, can be excluded from the fits (Table 1).

The a priori atmosphere used as an input to the retrieval algorithm was subdivided into 120 layers, from the ground (0.1 km) to 120 km. For the 45 lowest layers, from the ground to about 10 km, the pressure, temperature and relative humidity measurements from the PTU sondes were used as the a priori. For the higher altitudes, standard values corresponding to a mid-latitude, mid-summer atmosphere were taken into account except when values from the sondes were still available (up to 32 km on June 25). The relative humidity vertical profiles used for the 2 days of interest to this work are shown in Fig. 2. The water vapor line parameters were taken from the Hitran-formatted line lists of either HITRAN 2000, or the ESA or BR databases.

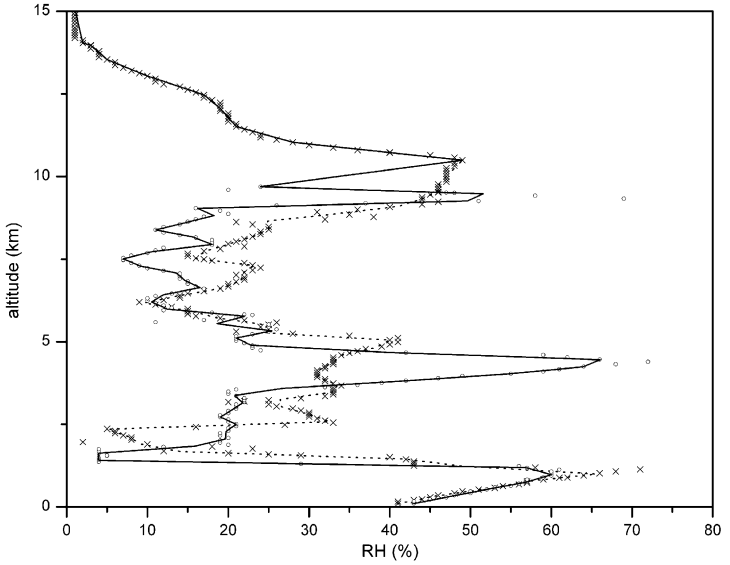

Fig. 2. Sonde measurements of relative humidity (Vaisala RS90 sonde) performed by KMI-IRM in Brussels on the 25th (crosses) and 26th (open circles) June 2001. The dotted and solid lines give the 45-points interpolation for both days, for input in the retrieval algorithm.

4. Results and discussion

4.1. Database comparisons

A detailed comparison of the three different line lists and other literature data was already given elsewhere [23]. Further comparisons between HITRAN and the ESA database can also be found in [7,8]. Here we only give a brief summary of these results, which focuses on the 14,000–18,000 cm^{-1} spectral region of interest to this work (Table 2). It should first be mentioned that in this spectral region, the ESA line list is considered as reliable only below 15,000 cm^{-1}, all line parameters at higher frequencies being provisional or originating from HITRAN. Also to note is the fact that the BR database has recently been updated with the measurement of air-broadening and air-shift parameters [31]. The updated line list, which will be discussed here only briefly, can also be found at the URL http://www.ulb.ac.be/cpm.

The most obvious difference between the HITRAN2000 and the BR databases is the number of lines: 5202 lines have been measured in BR using a very long absorption path (600 m), whilst 2481 are listed in HITRAN. Most of the newly identified lines in BR have an absorption cross-section smaller than 3.42×10^{-27} cm^{-1}/molecules cm^{-2}, which is the lowest value listed in HITRAN. In the ESA database, calculated values for many of the weaker lines have been added. Overall, the line positions agree well in the three line lists (the averaged standard deviation is smaller than 10^{-3} cm^{-1}), but differences up to 0.046 cm^{-1} are to be noted (Table 2). Significant disagreements exist for the line absorption cross-sections. This is discussed thoroughly in [23] but at this point it is, however, worth stressing again that the strongest lines in the 4ν polyad have a larger value

Table 2
Summary of spectroscopic parameters for water vapour between 14,000 18,000 cm^{-1}, as listed in the HITRAN 2000, the ESA and the BR databases

	Averaged value	Standard deviation	Minimum value	Maximum value	Sum	Number of values
Wave numbers v (cm^{-1})						
$v_{BR} - v_{HITRAN\ 2000}$	8.96×10^{-4}	0.006	−0.029	0.029	—	2397
$v_{ESA} - v_{HITRAN\ 2000}$	-4.71×10^{-4}	0.006	−0.046	0.040	—	2228
Cross-sections σ (cm^{-1}/molecules cm^{-2})						
HITRAN 2000	—	—	3.42×10^{-27}	6.45×10^{-24}	5.73×10^{-22}	2481
BR	—	—	4.47×10^{-28}	6.94×10^{-24}	5.72×10^{-22}	5202
ESA	—	—	3.42×10^{-30}	6.91×10^{-24}	6.02×10^{-22}	6987
$\sigma_{BR}/\sigma_{HITRAN\ 2000}$	0.89	0.28	—	—	—	—
$\sigma_{ESA}/\sigma_{HITRAN\ 2000}$	0.93	0.28	—	—	—	—
Self-broadening widths γ_{self} (cm^{-1} atm^{-1})						
HITRAN 2000	0.432	0.066	0.000	0.705	—	2481
BR	0.531	0.361	0.001	4.307	—	5202
ESA	0.370	0.093	0.000	0.806	—	6987
Air-Broadening widths γ_{air} (cm^{-1} atm^{-1})						
HITRAN 2000	0.086	0.013	0.022	0.110	—	2481
BR	0.079	0.034	0.001	0.915	—	5202
ESA	0.073	0.019	0.022	0.157	—	6987

(by about 5%) of their absorption cross-sections in the BR database as compared to HITRAN. The opposite conclusion was drawn for the weaker lines [23]. The self- and air-broadening parameters are in agreement to within 10% on average but care has to be taken by the fact that the values listed for these parameters are often default values, which can be significantly far from reality as a result of their strong dependency on the rotational and vibrational quantum numbers [32]. Although the use of default values for the self-broadening parameter will have little influence on the atmospheric calculations (about 2% error on the line width for a 20% uncertainty on γ_{self}), this will not be the case for the air-broadening parameter. In the BR database, it was decided to retain all measured γ_{air} values for which the fit to the observed spectrum was better than the fit using a default value, regardless if these measured values were unusually small or large.

For the sake of illustration, Fig. 3 shows simulated spectra of water vapor under 1 atm of air, using either the HITRAN 2000, the ESA or the BR database. Exception being made for a few lines, the agreement between the simulated spectra is better than 10%. A closer look at the residuals in a smaller spectral interval (14,400–14,450 cm^{-1}) reveals interestingly that part of the differences between HITRAN and BR comes from the line positions, whereas differences between HITRAN and ESA are mostly due to the line intensities (Fig. 3b).

4.2. Retrievals of atmospheric water vapor columns

The result of the fits of an atmospheric spectrum recorded on the 26th of June at noon UT (13h19 local time, solar zenith angle of 27.85°) using the water vapor line parameters listed in HITRAN 2000 is illustrated in Fig. 4, for the five different microwindows selected. The results of similar fits using the other databases are summarized in Table 3.

It is first to be noticed that in the spectral region above $15,000\ \mathrm{cm}^{-1}$, the HITRAN 2000 and the ESA databases provide similar results. This is not surprising as the parameters of the strongest lines in that spectral range are common to both databases. In the following, we will therefore concentrate

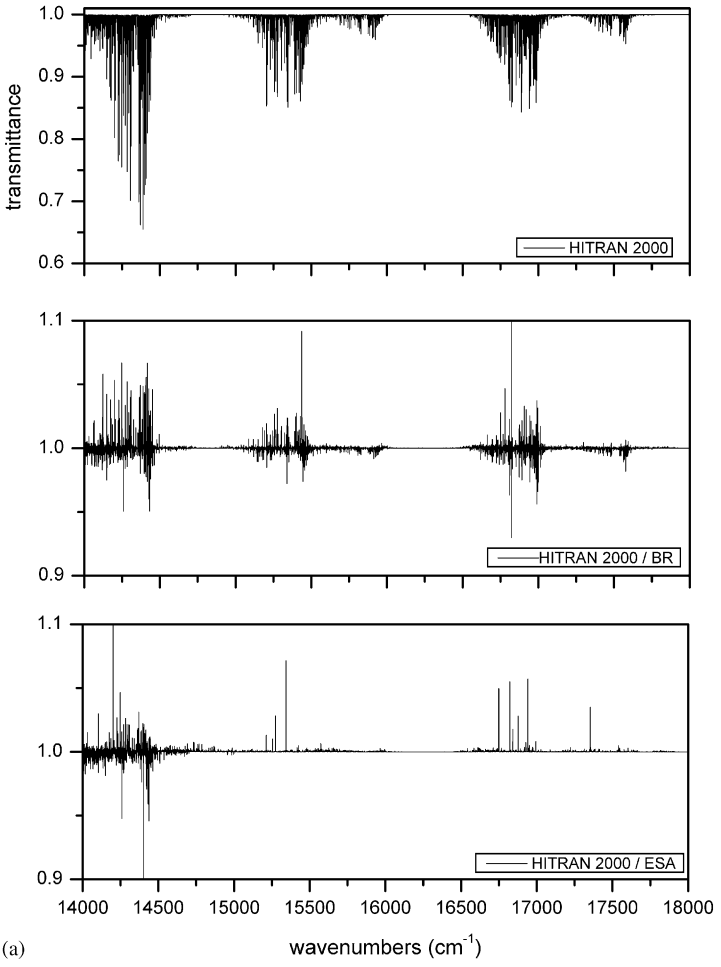

Fig. 3. Simulated water vapor transmittance spectrum using HITRAN 2000, under 1 atm at 296 K between (a) 14,000 and $18,000\ \mathrm{cm}^{-1}$ and (b) 14,400 and $14,450\ \mathrm{cm}^{-1}$. The bottom plots give the ratio of the simulated HITRAN spectrum with spectra simulated similarly with the BR and ESA databases.

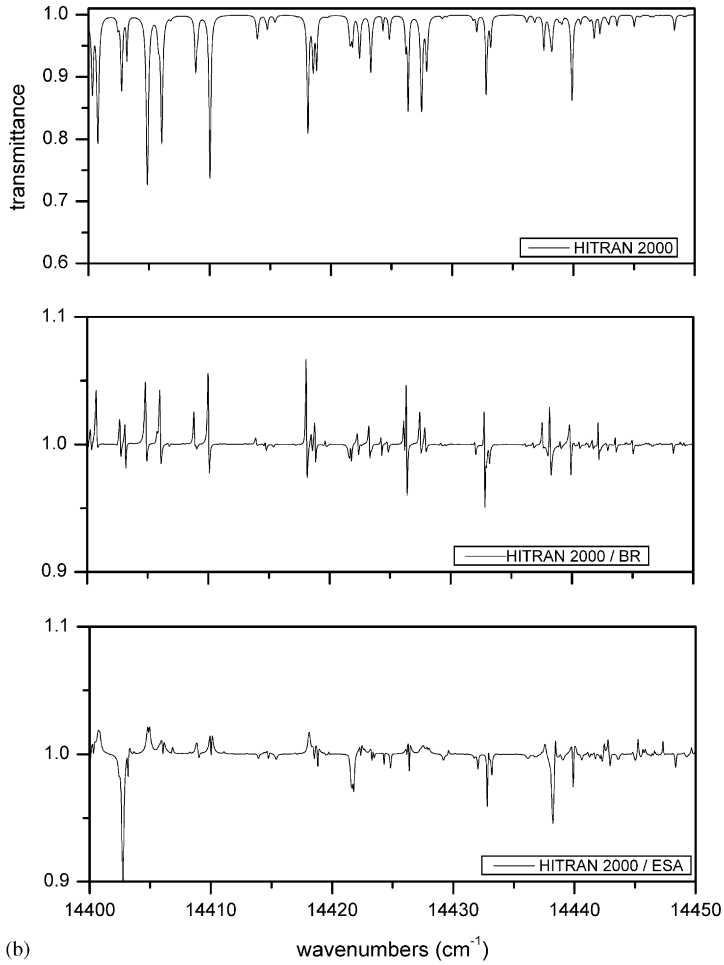

Fig. 3. *continued.*

our discussion on the comparison between HITRAN 2000 and BR, and highlight the results obtained with ESA when the latter are significantly different than those obtained using HITRAN.

In all the investigated atmospheric windows, the use of the BR database systematically improves the spectral fits when compared to HITRAN 2000. This is for instance indicated by the lower root-mean-squared (RMS) values in Table 3. It is also seen that the retrieved water vapor columns are lower than those obtained with HITRAN for all atmospheric windows except between 16,809.7 and $16,819.65\ \mathrm{cm}^{-1}$ (Table 3 and Fig. 5), with the differences being largest for the spectral region between 14,288.1 and $14,320\ \mathrm{cm}^{-1}$ (strong lines belonging to the 4ν polyad), and smallest for the region between 16,876.3 and $16,897.6\ \mathrm{cm}^{-1}$ (lines with a moderate intensity belonging to the 5ν polyad). An important result is obviously that the retrieved water column in the five different windows is much more consistent when using the BR database than when using HITRAN 2000 (Fig. 5). This shows the high homogeneity in the BR database, which was generated from experiments

performed during several consecutive days under stable experimental conditions, over an extended spectral range (8500–26,000 cm^{-1}). As for the comparison with the ESA database, it is to be pointed out that in the 14,288.1–14,320.0 cm^{-1} spectral region, the fits performed using ESA and BR are in excellent agreement (Table 3), both for the quality of the fits as for the retrieved water vapor column values ($[H_2O]_{ESA} = 6.32 \times 10^{22}$ molecules cm^{-2} and $[H_2O]_{BR} = 6.23 \times 10^{22}$ molecules cm^{-2}). This is interesting because the line parameters listed in ESA for the strongest lines in that spectral region

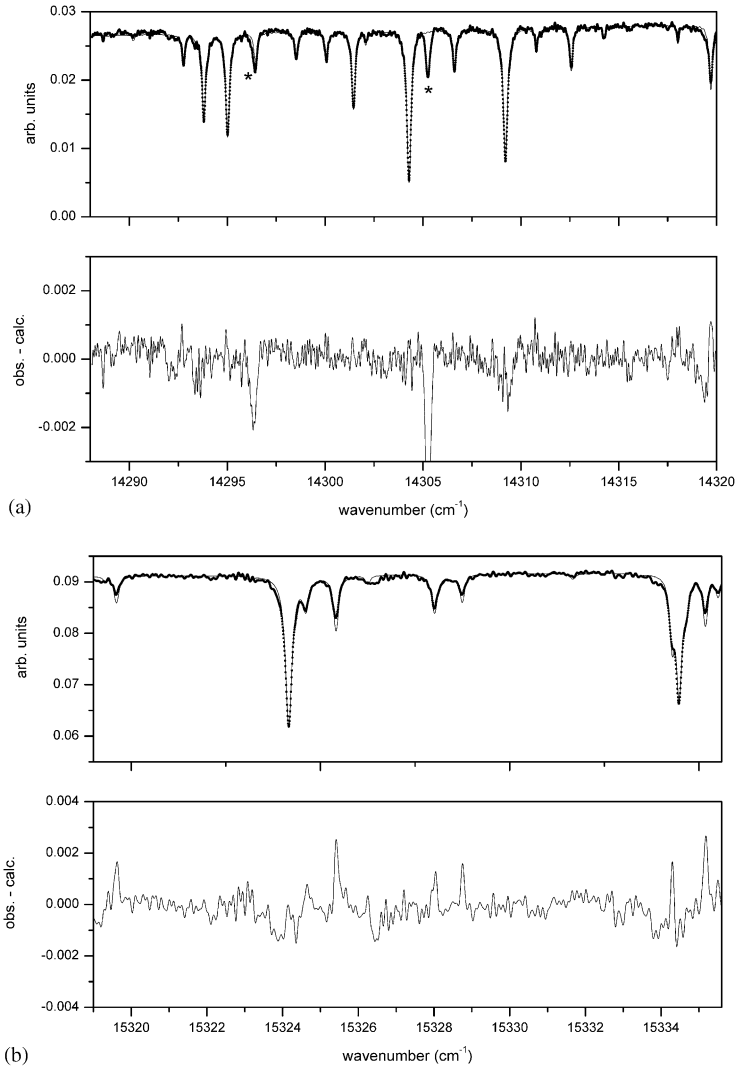

Fig. 4. Retrieval of water vapor total columns from the solar absorption spectrum measured at a zenith angle of 27.85° on the 26th of June 2001 (dots), in the five windows given in Table 1. The fitted spectra, obtained using the HITRAN 2000 database as the reference for water vapor are shown with the solid black lines. The strong solar lines are marked with an asterisk.

are experimental values. The agreement in the atmospheric calculations shows thus essentially the agreement between the experimental data in the two line lists. It should also be noticed that problems were encountered when fitting the spectrum with ESA in some spectral regions not presented here, as a result of a mismatch in the line positions between the measured spectrum and the calculated parameters.

The improvement when using the BR database in the atmospheric calculations instead of HITRAN 2000 is further highlighted in Fig. 6, where the calculations are shown for a spectrum recorded with a large solar zenith angle (SZA = 81.76°). In these conditions the absorption path in the troposphere is much larger and the weak water lines, which are not seen in spectra recorded at lower zenith angle,

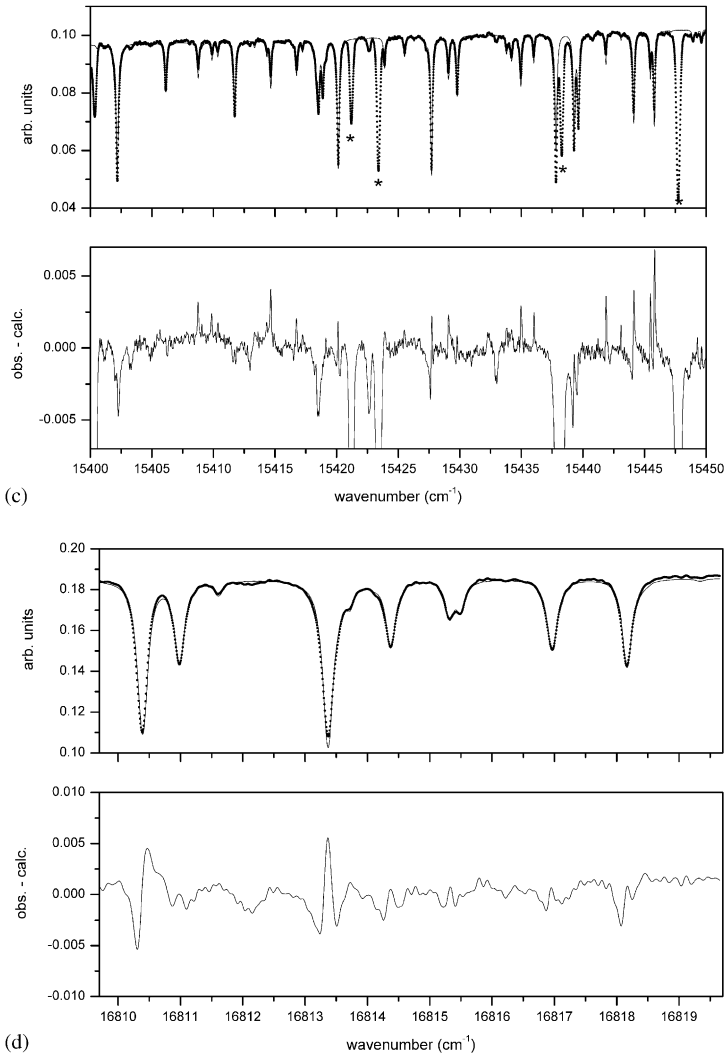

Fig. 4. *continued.*

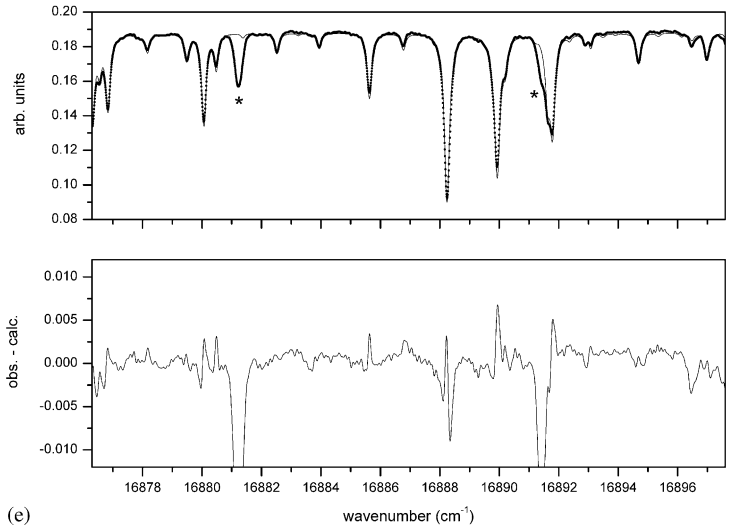

Fig. 4. *continued.*

contribute significantly. Many of these weak lines are not listed in HITRAN 2000 and the spectral fits using this database are therefore of reduced quality (Fig. 6a). At large solar zenith angles, the quality of the fits depends more on the differences in the line parameters for the strongest lines. Here we argue that this is partly due to the values of the air-broadening parameters listed in the databases. Indeed, most lines in HITRAN have been given calculated standard values of γ_{air}, which seem to be too small for modeling the high-pressure regions of the troposphere (Fig. 6a). In the BR database, the values of γ_{air} do not appear to be sufficiently well defined for reproducing the line profiles at higher pressures. It should therefore be reminded at this point that for the construction of the Hitran-formatted BR line list, the values of the air-broadening parameters were generated from the measured values of nitrogen-broadening parameters, by applying a constant correction to all lines [23]. The use of the updated BR line list, which includes new measurements of the air-broadening parameter, brings further improvements in the spectral fitting procedure (Fig. 6b). The latter should therefore be preferred in performing future atmospheric calculations.

In this discussion, it is also interesting to compare the results of the spectral fits using the different water line lists to an independent set of measurements. In Table 3, we compare the retrieved water vapor columns (WVC) measured at noon to the value given by the collocated PTU sondes for the 26th of June. The results show that when using the BR line list, the retrieved water vapor column agrees with the PTU measurements to within 3% for all microwindows. In all cases, the WVC is, however, slightly lower than that provided by the sondes. No such agreement is obtained with the other line lists, though it should be pointed out that the retrieved WVC still agree with the sondes measurements within the experimental errors. These results suggest that high-resolution visible Fourier transform spectroscopy offers an alternative method for monitoring the evolution of the atmospheric water vapor column over daytime. This can be seen in Fig. 7, where the retrieved water vapor columns from the spectra measured between 15,319 and $15,335.6\,cm^{-1}$ are

Table 3
Results of the retrieval of water vapor columns from the spectrum recorded at a solar zenith angle of 27.85° on the 26th of June 2001 (Fig. 4). WVC gives the total water vapor column, stdv the standard deviation (1σ), RMS the root-mean-squared value of the fit and ΔWVC the deviation with respect to the total column provided by the balloon-borne PTU sondes (6.33×10^{22} molecules cm^{-2})

	Atmospheric window 1 (14,288.1–14,320.0 cm^{-1})				Atmospheric window 2 (15,319.0–15,335.6 cm^{-1})				Atmospheric window 3 (15,400.0–15,450.0 cm^{-1})			
	WVC (molecules cm^{-2})	stdv	RMS	ΔWVC[a] %	WVC (molecules cm^{-2})	stdv	RMS	ΔWVC %	WVC (molecules cm^{-2})	stdv	RMS	ΔWVC %
HITRAN 2000	$6.83 \times 10^{+22}$	$1.08 \times 10^{+22}$	3.63×10^{-4}	8.0	$6.69 \times 10^{+22}$	$1.05 \times 10^{+22}$	4.99×10^{-4}	5.7	$6.52 \times 10^{+22}$	$1.53 \times 10^{+22}$	6.21×10^{-3}	3.0
BR	$6.32 \times 10^{+22}$	$9.78 \times 10^{+21}$	3.45×10^{-4}	−0.1	$6.15 \times 10^{+22}$	$6.62 \times 10^{+21}$	2.21×10^{-4}	−2.8	$6.22 \times 10^{+22}$	$1.11 \times 10^{+22}$	3.51×10^{-3}	−1.7
ESA	$6.23 \times 10^{+22}$	$8.81 \times 10^{+21}$	2.98×10^{-4}	−0.5	$6.68 \times 10^{+22}$	$1.04 \times 10^{+22}$	4.92×10^{-4}	5.5	$6.52 \times 10^{+22}$	$1.54 \times 10^{+22}$	6.35×10^{-3}	3.1
	Atmospheric window 4 (16,809.7–16,819.7 cm^{-1})				Atmospheric window 5 (16,876.3–16,897.6 cm^{-1})							
	WVC (molecules cm^{-2})	stdv	RMS	ΔWVC %	WVC (molecules cm^{-2})	stdv	RMS	ΔWVC %				
HITRAN 2000	$5.79 \times 10^{+22}$	$6.15 \times 10^{+21}$	2.02×10^{-3}	−8.5	$6.25 \times 10^{+22}$	$7.56 \times 10^{+21}$	4.08×10^{-3}	−1.3				
BR	$6.16 \times 10^{+22}$	$5.86 \times 10^{+21}$	1.65×10^{-3}	−2.7	$6.19 \times 10^{+22}$	$6.51 \times 10^{+21}$	3.10×10^{-3}	−2.2				
ESA	$5.79 \times 10^{+22}$	$6.19 \times 10^{+21}$	2.05×10^{-3}	−8.5	$6.06 \times 10^{+22}$	$8.56 \times 10^{+21}$	5.57×10^{-3}	−4.2				

[a]Calculated as $([WVC]_{retrieved} - [WVC]_{sondes})/[WVC]_{sondes}$.

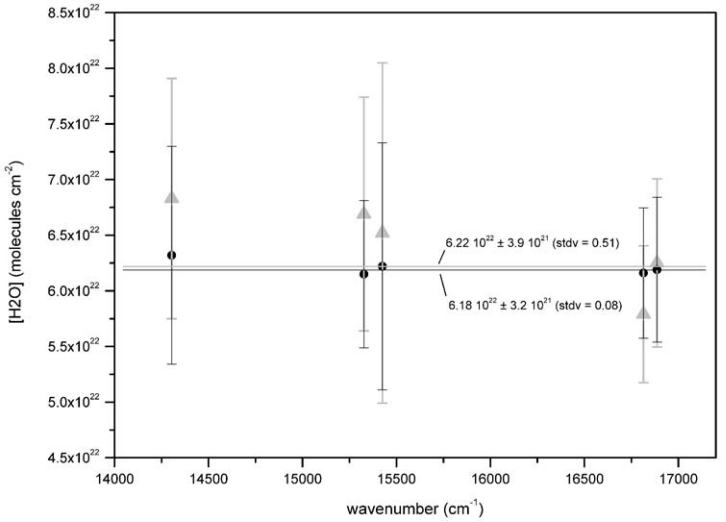

Fig. 5. Water vapor columns retrieved from the atmospheric windows given in Fig. 4, using HITRAN (grey triangles) and using BR (plain circles). Linear regressions weighted by the errors give the averaged value of the water vapor column, as well as the standard deviation (stdv).

plotted as a function of time and compared to the value of the PTU sondes at noon and those of the European Center for Medium Weather Forecasting at three different hours (ECMWF, personal communication).

5. Conclusion

In this work, we have investigated the reliability of different spectroscopic databases (HITRAN 2000, ESA and BR) for the measurement of atmospheric water vapor from spectra measured in the visible spectral region ($14{,}000–18{,}000\ \mathrm{cm}^{-1}$). For this purpose, spectra recorded by ground-based high-resolution Fourier transform spectrometers in June 2001 in Brussels have been analyzed by means of inverse models. It is shown that the use of the BR database in the atmospheric models allows a better reproduction of the atmospheric spectra than the HITRAN 2000 database, especially at large zenith angles, where the weak lines contribute significantly and where accurate values of air-broadening parameters are needed. A good agreement between the BR and the ESA databases is reported for spectral regions in which experimental values of the line parameters are available in both databases. When compared to in situ measurements performed simultaneously by PTU sondes, it is shown that all databases provide a good agreement within the error bars. The BR database gives, however, the closest agreement. With the latter, we have also been able to monitor the daily variations of the atmospheric water vapor amount during daytime. These results suggest a potential use of ground-based high-resolution Fourier transform spectroscopy for monitoring the variability of atmospheric water vapor. As the determination of vertical profiles is more particularly needed for climate oriented studies, it will be important to undertake further studies in order to

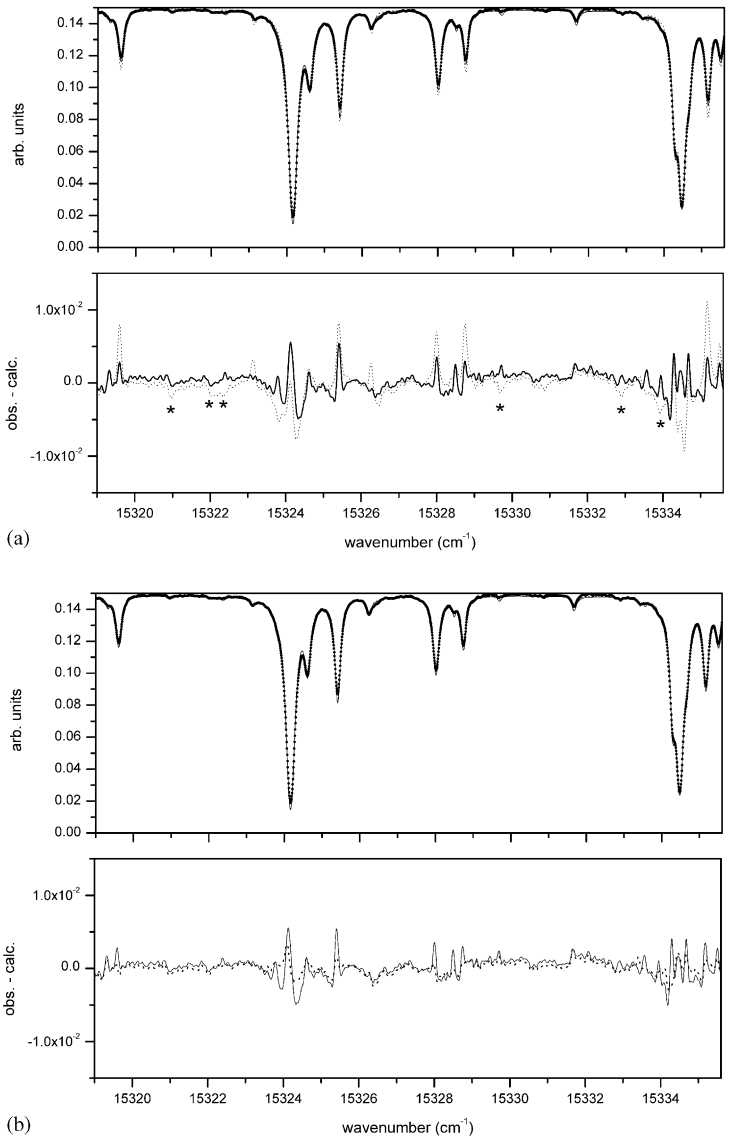

Fig. 6. Retrieval of the water column from a spectrum measured at large zenith angle (81.76°) on the 25th of June (dots), using (a) HITRAN (dotted line) and BR (solid line) and (b) BR (solid line) and the updated list with measured air-broadening parameters (dotted line). In the residuals of Fig. 6a, asterisks are used to mark some of the weak lines not listed in HITRAN. The RMS values of the fits are the following: RMS[HITRAN 2000] $= 0.10 \times 10^{-1}$, RMS[BR] $= 0.33 \times 10^{-2}$, RMS[updated BR] $= 0.12 \times 10^{-2}$

determine the possibilities that high-resolution FT visible spectroscopy can offer for this purpose. Further improvements in the knowledge of the water vapor spectroscopic parameters, especially with regard to the dependency on the pressure and temperature, will undoubtedly be needed for that purpose.

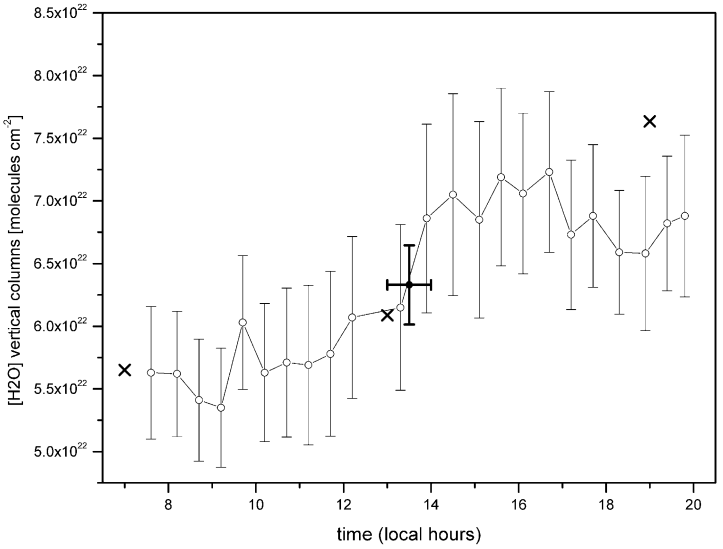

Fig. 7. Evolution of the water vapor column retrieved for June 26 from FT-visible spectra in the 15,319–15,335.6 cm^{-1} spectral region, using the BR database (open circles). The plain circle gives the value of the PTU sonde and the black crosses the values provided by the European Center for Medium Weather Forecasting (ECMWF, personal communication).

Acknowledgements

The authors would like to acknowledge P.F. Bernath (University of Waterloo, Canada) for useful discussions and comments. This research was funded by the Belgian State, Federal Offices for Scientific, Technical and Cultural Affairs, the Fonds National de la Recherche Scientifique (FNRS, Belgium) and the European Space Agency (contract 14145/00/NL/SFe(IC)). Marco Matricardi is acknowledged for providing the ECMWF vapor profiles, which have been obtained within the framework of the ISSWG (IASI Sounding Science Working Group).

References

[1] Bernath PF. The spectroscopy of water vapour: Experiment, theory and applications. Phys. Chem. Chem. Phys. 2002;4(9):1501–9.
[2] Ramanathan V, Vogelmann AM. Greenhouse Effect, Atmospheric Solar Absorption and the Earth's radiation budget: From the Arrhenius-Langley Era to the 1990's. Ambio 1997;26(1):38–46.
[3] Camy-Peyret C, Flaud J-M, Mandin J-Y, Chevillard J-P, Brault J, Ramsay DA, Vervloet M, Chauville J. The high-resolution spectrum of water vapor between 16500 and 25250 cm^{-1}. J. Mol. Spec. 1985;113:208–28.
[4] Mandin J-Y, Chevillard J-P, Camy-Peyret C, Flaud J-M. J. Mol. Spec. 1986;116:167–90.
[5] Carleer M, Jenouvrier A, Vandaele AC, Bernath PF, Mérienne M-F, Colin R, Zobov NF, Polyansky OL, Tennyson J, Savin SA. The near infrared, visible, and near ultraviolet overtone spectrum of water. J. Chem. Phys. 1999;111(6):2444–50.
[6] Zobov NF, Belmiloud D, Polyansky OL, Tennyson J, Shirin SV, Carleer M, Jenouvrier A, Vandaele AC, Bernath PF, Mérienne M-F, Colin R. The near ultraviolet rotation-vibration spectrum of water. J. Chem. Phys. 2000;113(4):1546–52.

[7] Schermaul R, Learner RCM, Newnham DA, Williams RG, Ballard J, Zobov NF, Belmiloud D, Tennyson J. The water vapor spectrum in the region 8600-15000 cm^{-1}: Experimental and theoretical studies for a new spectral line database: I. Laboratory measurements. J. Mol. Spec. 2001;208:32–42.
[8] Schermaul R, Learner RCM, Newnham DA, Ballard J, Zobov NF, Belmiloud D, Tennyson J. The water vapor spectrum in the region 8600-15000 cm^{-1}: Experimental and theoretical studies for a new spectral line database: II. Linelist construction. J. Mol. Spec. 2001;208:43–50.
[9] Cheng JX, Lin H, Hu SM, He SG, Zhu QS, Kachanov A. Infrared intracavity laser absorption spectroscopy with a continuous scan Fourier-transform interferometer. Appl. Opt. 2000;39(13):2221–9.
[10] Guelachvili G. Time-resolved spectroscopy of stable molecules. Vib. Spectroscopy 2002;29(1-2):21–6.
[11] Naus H, Ubachs W, Levelt PF, Polyanski OL, Tennyson J. cavity-ring-down spectroscopy on water vapor in the range 555-604 nm. J. Mol. Spec. 2001;205(1):117–21.
[12] Kalmar B, O'Brien JJ. Quantitative intracavity laser spectroscopy measurements with a Ti:sapphire laser; Absorption intensities for water vapor lines in the 790-800 nm region. J. Mol. Spec. 1998;192:386–93.
[13] Harder JW, Brault JW. Atmospheric measurements of water vapor in the 442 nm region. J. Geophys. Res. 1997;102(D5):6245–52.
[14] Grossmann BE, Browell EV. Water-vapor line broadening and shifting by air, nitrogen, oxygen, and argon in the 720-nm wavelength region. J. Mol. Spec. 1989;138:562–95.
[15] Grossmann BE, Browell EV. Spectroscopy of water-vapor in the 720-nm wavelength region: Line strengths, self-induced pressure broadenings and shifts, and temperature dependence of linewidths and shifts. J. Mol. Spec. 1989;136:264–94.
[16] Giver LP, Chackerian Jr C, Varanasi P. Visible and near-infrared $H_2{}^{16}O$ line intensity corrections for HITRAN-96. J. Quant. Spectrosc. Radiat. Transfer 2000;66:101–5.
[17] Rothman LS, Barbe A, Benner C, Brown LR, Camy-Peyret C, Carleer M, Chance KV, Clerbaux C, Dana V, Devi M, Fayt A, Fischer J, Flaud J-M, Gamache RB, Goldman A, Jaquemart D, Jucks KW, Lafferty W, Mandin J-Y, Massie ST, Newnham D, Perrin A, Rinsland CP, Schroeder J, Smith K, Smith MA, Toth RA, Vander Auwera J, Varanasi P, Yoshino K. The HITRAN Molecular Spectroscopic Database: 2000 Edition. J. Quant. Spectrosc. Radiat. Transfer 2003; doi:10.1016/S0022-4073(03)00146-8.
[18] Learner RCM, Zhong W, Haigh JD, Belmiloud D, Clarke J. The contribution of the unknown weak water vapor lines to the absorption of solar radiation. Geophys. Res. Lett. 1999;26(24):3609–12.
[19] Chagas JCS, Newnham DA, Smith KM, Shine KP. Effects of improvements in near-infrared water vapour line intensities on short-wave atmospheric absorption. Geophys. Res. Lett. 2001;28(12):2401–4.
[20] Arking A. Absorption of solar energy in the Atmosphere: Discrepancy between model and observations. Science 1996;273:779–81.
[21] Lang R, Maurellis AN, van der Zande W, Aben I, Landgraf J, Ubachs W. Forward modeling and retrieval of water vapor from GOME: Treatment of narrow band absorption spectra. J. Geophys. Res. 2002; 107(D16): article 4300.
[22] Maurellis AN, Lang R, van der Zande W, Aben I, Ubachs W. Precipitable water vapor column retrieval from GOME data. Geophys. Res. Lett. 2000;27(6):903–6.
[23] Coheur P-F, Fally S, Carleer M, Clerbaux C, Colin R, Jenouvrier A, Mérienne M-F, Hermans C, Vandaele AC. New water vapor line parameters in the 26000-13000 cm^{-1} region. J. Quant. Spectrosc. Radiat. Transfer 2002;74: 493–510.
[24] Bennartz R, Lohmann U. Impact of improved near infrared water vapor line data on absorption of solar radiation in GCMS. Geophys. Res. Lett. 2001;28(24):4591–4.
[25] Lubin D, Vogelmann A, Lehr PJ, Kressin A, Ehramjian J, Ramanathan V. Validation of visible/near-IR atmospheric absorption and solar emission spectroscopic models at 1 cm^{-1} resolution. J. Geophys. Res. 2000;105(17):22445–54.
[26] Smith KM, Newnham DA. High-resolution atmospheric absorption by water vapor in the 830-985 nm region: Evaluation of spectroscopic databases. Geophys. Res. Lett. 2001;28(16):3115–8.
[27] Veihelmann B, Lang R, Smith KM, Newnham D, van der Zande WJ. Evaluation of spectroscopic databases of water vapor between 585 and 600 nm. Geophys. Res. Lett. 2002;29(15):10.129/2002GL015330.
[28] Gallery WO, Kneizys FX, Clough SA. Air mass computer program for atmospheric transmittance/radiance calculation: FSCATM. AFGL-TR-83-0065 1983; ADA132108.
[29] Zander R, Demoulin P, Mahieu E, Adrian GP, Rinsland CP, Goldman A. ESLMOSII/NDSC-IR spectral fitting algorithms intercomparison exercise, Proceedings of the ASA '93 Workshop, Reims, France, 1994. p. 7–12.

[30] Press WH, Teukolsky SA, Vetterling WT, Flannery BP. Numerical recipes in Fortran 77: The art of scientific computing. Melbourne, Australia: Cambridge University Press, 1996.
[31] Fally S, Coheur P-F, Carleer M, Clerbaux C, Colin R, Jenouvrier A, Mérienne M-F, Hermans C, Vandaele AC. Water vapor line broadening and shifting by air in the 26000-13000 cm^{-1} region. J. Quant. Spectrosc. Radiat. Transfer 2003; doi:10.1016/S0022-4073(03)00149-3.
[32] Hartmann J-M, Gamache RR. Collisional parameters of H_2O lines: effects of vibration. J. Quant. Spectrosc. Radiat. Transfer 2003; in press.